NISTIR 7429

Thermo-viscoelastic Analysis of Ambient Cure Epoxy Adhesives Used in Construction Applications

Joannie Chin
Don Hunston
Aaron Forster

NIST
National Institute of Standards and Technology
Technology Administration, U.S. Department of Commerce

NISTIR 7429

Thermo-viscoelastic Analysis of Ambient Cure Epoxy Adhesives Used in Construction Applications

Joannie Chin, Don Hunston and Aaron Forster
Polymeric Materials Group
Materials and Construction Research Division
Building and Fire Research Laboratory

U.S. DEPARTMENT OF COMMERCE
Carlos M. Gutierrez, Secretary
TECHNOLOGY ADMINISTRATION
Robert C. Cresanti, Under Secretary of Commerce for Technology
NATIONAL INSTITUTE OF STANDARDS AND TECHNOLOGY
William Jeffrey, Director

Thermo-viscoelastic Analysis of Ambient Cure Epoxy Adhesives Used in Construction Applications

Joannie Chin, Donald Hunston and Aaron Forster
Polymeric Materials Group
Materials and Construction Research Division
National Institute of Standards and Technology

Abstract

The thermo-viscoelastic properties of two commercial, ambient cure structural epoxy adhesives were analyzed and compared. The adhesives were formulated by the same manufacturer, but one system contained accelerators to shorten its cure time. The long term tensile creep compliance of the two systems was estimated by applying the Ninomiya and Ferry method to dynamic mechanical master curves generated using time-temperature superposition. Differential scanning calorimetry (DSC) and thermogravimetric analysis (TGA) were used to assess the thermal properties of the materials following ambient processing as well as after moisture saturation. Differences were observed in the dynamic mechanical, thermal, and hydrolytic properties of the two adhesive systems as well as in their estimated creep compliance behavior, which were attributed to differences in the curing agent(s) and accelerator(s) used in the adhesive systems.

Introduction

In building and construction applications, ambient cure structural adhesives are used for adhesive grouting of bolts and other inserts into cured concrete [1], bonding of steel or fiber-reinforced composite reinforcing plates to bridge decks [2], and seismic retrofitting of concrete columns [3]. These thermoset materials are typically packaged as two-part systems with the base resin in one container and one or more curing agents, catalysts, and/or accelerators in the other. Base resins commonly used in these systems are epoxy, isophthalic polyester and vinyl ester, combined with the appropriate curing agents. Other ingredients could include flow control agents and/or inorganic fillers such as silica, titanium dioxide, or calcium carbonate.

The contents of the two containers are typically combined at the point of use via hand-mixing or with a self-mixing cartridge gun. When the components come into contact with each other, a curing reaction is initiated involving the formation of chemical bonds between the reactive groups in the base resin and curing agent(s). The viscosity of the mixture begins to rise as the curing reaction proceeds, a result of molecular weight increase occurring via an increase in chain length and/or by the formation of linkages between chains to produce a network structure. At some point, the networks become large enough that they traverse the entire sample, and the system is said to have reached *gelation* [4]. At gelation, the material is elastomeric, but there is still sufficient molecular mobility for the reactions to continue.

Eventually, the molecular structure reaches *vitrification*, a stage of cure at which the material becomes a rigid, glassy solid. At this point, the molecular mobility of the material is so low that it is very difficult for reactive groups to diffuse to each other, and thus the curing process essentially stops. Vitrification normally occurs before all of the available groups have reacted, and thus most thermoset materials are not fully cured (i.e.

100 % of the possible reactive groups are not consumed). Higher cure temperatures permit the reaction to continue further before vitrification, thus leading to a higher degree of cure, but at some point thermal degradation begins. Consequently, it is difficult to find a temperature that is high enough to produce a fully cured material. If a sample is heated above its T_g in a process known as postcuring, the material may de-vitrify and unreacted groups will again have a chance to react and further advance the degree of cure.

Adhesives formulated to cure at ambient conditions often react exothermically, so that the actual temperature of the material during the cure process may be higher than ambient. Nevertheless, these materials might have a lower degree of cure than elevated temperature cured systems, and this could produce unexpected properties. Moreover, they may be used at temperatures close to their T_g, which could affect their thermal, hydrolytic, and long-term mechanical properties, particularly under sustained loading and/or severe environments.

Most of the published literature has focused on elevated temperature cure epoxy systems; hence, there is a lack of data on the properties of ambient cure systems. This study seeks to characterize the thermo-viscoelastic properties of two commercial, ambient cure structural epoxy adhesives using dynamic mechanical thermal analysis, differential scanning calorimetry and thermogravimetric analysis. The long term tensile creep compliance of the two systems was estimated by applying the Ninomiya and Ferry method to dynamic mechanical master curves generated using time-temperature superposition.

Experimental Procedure *

Materials

Two commercial ambient cure structural epoxy adhesive systems were selected for this study. Both adhesives were formulated by the same manufacturer and were purchased from the same commercial industrial supplier. These adhesives are hereinafter referred to as "Epoxy A" and "Epoxy B." Relative to Epoxy B, Epoxy A was formulated by the manufacturer to have reduced gel and cure times. The Material Safety Data Sheets (MSDS) for the base resin in both Epoxy A and Epoxy B were the same, listing a proprietary epoxy resin, calcium carbonate and talc. The MSDS information showed that the curing agent formulations for the two systems differed: While both contained calcium carbonate and talc filler, Epoxy A contained aliphatic amines, benzyl alcohol, nonyl phenol, and phenol as major components, and Epoxy B contained aliphatic and cycloaliphatic amines, aromatic hydrocarbons and benzyl alcohol. Phenols in general, and particularly nonyl phenol, are commonly used accelerators in epoxy adhesives [5].

Specimen Preparation

Using a double-cartridge manual caulk gun supplied by the adhesive manufacturer, the two components were ejected from their respective cartridges, proportionally mixed with a static-element mixing nozzle and deposited onto fluoropolymer-coated release paper. The deposited adhesive was drawn down into a uniform film with a steel draw-down bar having a 1.25 mm gap. Films were allowed to

* Certain commercial equipment, instruments or materials are identified in this paper in order to specify the experimental procedure adequately. Such identification is not intended to imply recommendation or endorsement by the National Institute of Standards and Technology, nor is it intended to imply that the materials or equipment identified are necessarily the best available for this purpose.

cure under laboratory conditions (nominally 21 ^{o}C and 25 % RH) for a minimum of 72 h before analysis. Cured film thicknesses ranged from 0.19 mm to 0.30 mm. In order to check reproducibility between lots, two separate packages of each adhesive system (manufactured at different times) were used to produce sets of specimens for testing. Similar properties were observed in the specimens produced from the different lots.

It should be noted that in the room temperature processing of thin film specimens, any heat evolved during the cure process would be quickly dissipated and the temperature of the film would not rise significantly. In larger, bulkier components, however, the cure exotherm could potentially cause a significant temperature rise in the material, thus potentially causing the degree of cure to be more advanced compared to a thinner component.

Post-processing Exposure

Post-curing—Due to anomalies that were observed during preliminary analysis, one set of Epoxy A specimens from one lot was subjected to a 4 h post-cure at 60 ^{o}C in a circulating air oven in an attempt to increase the extent of cure.

Moisture Saturation—A portion of the Epoxy A and Epoxy B samples (representing samples from both lots) were exposed to a 22 ^{o}C/100 % RH environment to determine the effects of moisture sorption on their thermal and dynamic mechanical properties. This exposure consisted of suspending pre-cut specimens over a reservoir of distilled water in a screw-top glass container for a minimum of 72 h. Equilibrium mass uptake of moisture was crudely calculated by taking specimens out of the container and weighing them on an analytical balance until there were no additional changes in mass. Dynamic mechanical thermal analysis (DMTA) was then carried out on the saturated specimens, taking care to minimize the time between the removal of the specimens from

the high moisture environment and the beginning of the analysis. One set of saturated specimens was dried by storing them in open containers in the laboratory environment until their original dry mass was reached, and then analyzed via DMTA to determine whether the observed moisture effects were reversible.

Fourier Transform Infrared Spectroscopy (FTIR)

Infrared analysis of the cured epoxy films was carried out using a Nicolet Nexus FTIR equipped with a mercury-cadmium-telluride (MCT) detector and a SensIR Durascope attenuated total reflectance (ATR) accessory. Dry air was used as the purge gas. Consistent pressure on the films was applied using the force monitor on the Durascope. Three replicate spectra for each sample were recorded between 4000 cm^{-1} and 700 cm^{-1} and were averaged over 128 scans. Standard uncertainties associated with this measurement are ± 1 cm^{-1} in wavenumber and ± 1 % in peak intensity. In this report, spectra are presented in the range between 4000 cm^{-1} and 800 cm^{-1}, due to detector limitations below 800 $cm^{-1.}$

Differential Scanning Calorimetry (DSC)

Samples of the cured epoxy adhesives were sealed in aluminum pans and analyzed in a DSC 2910 (TA Instruments) differential scanning calorimeter equipped with a refrigerated cooling system. Analysis was conducted in a nitrogen atmosphere, in modulated DSC mode with a modulation frequency of ± 1 °C per 60 s. Samples were ramped from 0 °C to 60 °C for Epoxy A, and from 0 °C to 95 °C for Epoxy B, at a heating rate of 3 °C/min, then cooled to 0 °C at a rate of 3 °C/min. This sequence was then repeated in a second cycle. The T_g was determined by the half-height method in the first heating curve and first cooling curve. The relative standard uncertainty in the heat

flow measurements is typically ± 3 %, and the standard uncertainty in the temperature scale is typically ± 0.2 ^{o}C.

Thermogravimetric Analysis (TGA)

TGA was carried out on a TA Instruments 2950 high resolution thermo-gravimetric analyzer. Specimens having a nominal mass between 15 mg and 20 mg were placed in ceramic sample pans. Samples were equilibrated at 25 ^{o}C for 5 min, and then ramped to 500 ^{o}C at 5 ^{o}C/min. Analyses were carried out in a nitrogen atmosphere. The relative standard uncertainty in the mass measurements is typically ± 0.1 %, and the standard uncertainty in the temperature scale is typically ± 0.1 ^{o}C

Dynamic Mechanical Thermal Analysis (DMTA)

Specimens were cut with a razor blade into 5.3 mm x 20 mm strips and tested in tensile mode on a Rheometrics Solids Analyzer (RSA) III. Specimens were consistently tightened in the instrument grips using a torque wrench set to 20 cN·m. In order to establish the linear viscoelastic (LVE) region of the epoxy systems, tensile strain sweeps were conducted between 0.001 % and 1 % strain at room temperature and at a frequency of 10 Hz. A tensile pre-load of 100 g was used to prevent the specimens from buckling. A representative room temperature strain sweep for both epoxy systems is shown in Figure 1, in which log storage modulus (E') is plotted versus strain. Because the specimens (Epoxy A in particular) tended to be brittle, the majority of specimens failed at strains of ≤ 0.2 % in the strain sweep experiments. Strain sweeps were also carried out at 75 ^{o}C, to ensure that the materials did not exhibit non-linear viscoelastic behavior in the rubbery region. A test strain of 0.01 %, which is within the LVE domain at both room temperature and elevated temperature, was chosen for the remainder of the experiments.

Temperature sweeps were carried out from 5 ^{o}C to 100 ^{o}C, using a ramp rate of 5 ^{o}C/min, a frequency of 5 Hz and strain of 0.01 %. A tensile pre-load of 100 g was used to prevent the specimens from buckling. The dynamic mechanical glass transition temperature was taken as the peak of the loss modulus (E") curve, in accordance with ASTM E 1640-04 [6]. A minimum of three replicates were tested for each epoxy system. For the RSA III, the manufacturer-stated relative standard uncertainty in the force measurement is typically ± 0.0002 g, and the standard uncertainty in the temperature scale is typically ± 0.5 ^{o}C.

Data for time-temperature superposition were generated by conducting combined temperature/frequency sweeps at a strain of 0.01 %, from 0.005 Hz to 10 Hz and from 20 ^{o}C to 90 ^{o}C, using five different frequencies in each decade and at temperature intervals of 3 ^{o}C.

Time-Temperature Superposition

The dynamic mechanical data were analyzed for the applicability of time-temperature superposition. A software program developed previously by Hunston et al. [7] was used. The program takes E' and tan delta data from DMTA temperature/frequency sweeps and computes E', E" and tan delta master curves as a function of frequency. Tan delta and E' curves at each temperature are shifted horizontally along the frequency axis with respect to the 20 ^{o}C data to obtain the best visual overlap of the tan delta data. A small vertical shift is then applied to achieve the optimum overlap of the E' curves, if needed. It is assumed that, since tan delta is the ratio of E" and E', any vertical shift in the moduli would cancel out so only horizontal shifts are needed for tan delta data. This procedure reduces the ambiguity present when both horizontal and vertical shifts are being applied. The program also has the capability

to generate creep compliance curves from the dynamic mechanical master curves, using the approximation of Ninomiya and Ferry [8].

Results and Discussion

FTIR Analysis

The FTIR spectra of as-processed Epoxy A and Epoxy B are compared in Figure 2. A peak at 911 cm^{-1} corresponding to the epoxide ring is observed in the spectrum of Epoxy A, indicating that it contained unreacted epoxide functional groups. No epoxide ring peak was observed in the spectrum of Epoxy B. This observation suggests that, assuming that the two systems have similar base resin/curing agent stoichiometry, Epoxy A is less fully cured than Epoxy B when processed under ambient conditions. Also contained in this figure is the FTIR spectrum of Epoxy A following elevated temperature postcuring, in which the epoxide ring peak is no longer visible, indicating that elevated temperature treatment caused the curing process to proceed further, as discussed earlier.

Thermal Analysis

As-made Specimens— The T_g of a crosslinked network is an important experimental parameter that is correlated with the extent of cure or crosslinking [9]. Glass transition temperatures of the cured systems were measured using both DSC and DMTA; TGA was utilized to assess the overall thermal stability of the cured systems. Table 1 summarizes data from DSC, TGA and DMTA for both materials.

Figure 3 shows representative TGA curves for Epoxy A and Epoxy B. For Epoxy A, the onset of initial mass loss occurred at 75 ^{o}C, compared to 115 ^{o}C for Epoxy B.

These temperatures are far below the temperatures needed to disrupt most organic bonds; thus, the mass loss is most likely attributed to the volatilization of low-molecular weight, non-network components. The lower onset temperature for Epoxy A may be attributed to the presence of accelerator and/or the different curing agents used. The primary decomposition event involving breakage of common bonds founds in organic molecules (carbon-carbon, carbon-oxygen, carbon-nitrogen) occurred between 340 ^{o}C and 350 ^{o}C for both systems.

The initial mass loss onset temperature was used to establish the endpoint of the DSC experiments for each epoxy system. Representative modulated DSC reversing heat flow curves are shown in Figure 4. The first heat T_g of Epoxy B was observed to be slightly higher than that of Epoxy A. During the cooling step after the first heating cycle, Epoxy A exhibited a small but reproducible decrease in T_g, with no additional changes in T_g observed in the second heating and cooling cycles. No changes in the T_g of Epoxy B were observed following either the first or second heating/cooling cycles.

Changes in T_g of thermoset materials during DSC analysis can occur following the first heating cycle, and are attributed to thermal post-curing [9]. This phenomenon is not uncommon for ambient-cure systems, which contain may contain unreacted functional groups as seen in the FTIR analysis discussed earlier. If the material is exposed to temperatures above $T_{g,}$ the mobility of the reactive groups is restored and crosslinking can continue, sometimes evidenced by the appearance of a residual cure exotherm in the DSC curve. No such peaks were observed in the DSC analysis of Epoxy A, however, it is possible that the amount of heat released was very small and the exotherm intensity may be below the resolution of the instrument. Nevertheless, in the great majority of cases, the T_g of the post-cured material is shifted towards *higher* temperature, not *lower*, as observed in this study for Epoxy A.

Figure 5 shows the E’, E” and tan delta curves as a function of temperature for Epoxies A and B. The E’ curve distinctly shows the three regions of viscoelastic behavior - glassy, transition, and rubbery - that are characteristic of crosslinked amorphous polymers. As measured by the peak of the E” curve, the dynamic mechanical T_gs of Epoxy A and B are 50.3 ^oC and 52.5 ^oC, respectively, which are within (3 to 5) ^oC of first heat T_g values measured via DSC.

The storage moduli of the two systems in the vicinity of 30 ^oC are approximately equivalent, as would be expected for glassy materials. However, the rubbery modulus measured at 100 ^oC for Epoxy A is approximately 10 MPa while that of Epoxy B is 46 MPa. The lower rubbery modulus of Epoxy A might be attributed to factors such as lower crosslink density or lower filler content and would be expected to influence long term creep effects under the right conditions.

It was also noted that for both materials, the width of the E’, E” and tan delta transitions were greater than those typically observed for simple epoxies. The tan delta peak for Epoxy A also appeared to contain overlapping peaks. These results indicate that these materials are more complex and heterogeneous than simple thermosets; therefore, there is a broader range of response times for the molecular motions associated with the glass transition. This can happen when there is a mixture of epoxies or curing agents in a material giving rise to complex or multiple network structures. If the components are very different and distinct, such as in a phase-separated system, separate transition peaks are seen. If the components are similar or not phase-separated, the tan delta can show a broad peak with contributions from each component [10]. Fillers can produce a similar result: In a review of pigment effects on coating properties [11], the width of the tan delta peak was reported to be greater for a pigment-filled coating relative to its non-filled counterpart. Therefore, the presence of the inorganic fillers can contribute to the breadth

of the tan delta peak in the epoxy adhesives used in this study.

As illustrated in Figure 6, during the dynamical mechanical analysis the rubbery modulus for Epoxy A (E' curve > 85 ^{o}C) increased as a function of test temperature, reached a maximum at approximately 140 ^{o}C and then decreased. The increase in the rubbery modulus at elevated temperature might be the result of an increase in the crosslink density of the network [12], and when taken with the FTIR results discussed earlier, support the hypothesis that Epoxy A is not fully cured when processed at ambient temperature. The decrease in rubbery modulus at still higher temperatures could be due to thermal degradation of some component of the network.

Post-cured specimens—As discussed earlier, Epoxy A may have vitrified early in the curing process and remained undercured, possibly due to the presence of accelerators that decreased its cure time. To follow up on this possibility, DMTA temperature sweeps were carried out after specimens were post-cured at 60 ^{o}C for 4 h. This temperature was chosen for post-curing because it is above the T_g but below the onset of mass loss observed via TGA. As seen in Figure 7, a decrease in the T_g (peak of E" curve) following post-cure is observed, similar to the decrease in T_g following the first heating cycle in the DSC analysis. As discussed earlier, this behavior is unusual in that most elevated temperature post-curing operations tend to initiate additional polymerization or crosslinking in the network, which in turn increases the T_g. At the present time, the reasons for this unexpected behavior are not understood and speculations will be avoided, particularly in the light of the proprietary nature of the epoxy formulations. The behavior of specimens post-cured at higher temperatures was not investigated, and could differ from the specimens post-cured at 60 ^{o}C.

Moisture-saturated specimens—Test specimens were flexible and rubbery following exposure to a high relative humidity environment, in contrast to the brittleness

of the as-prepared specimens. Equilibrium moisture mass uptake values for the saturated epoxies relative to their dry mass were approximately 4.4 mass % for Epoxy A and 2.3 mass % for Epoxy B. Samples were not dried prior to the moisture exposure, thus any moisture already present in the specimens under ambient conditions was not accounted for in this calculation.

DMTA analyses of saturated Epoxy A and Epoxy B are shown in Figures 8 and 9, respectively. The T_g of Epoxy A decreased to 15 ^oC following moisture exposure; upon drying of the saturated specimens, the original T_g of 50 ^oC was recovered. Epoxy B also exhibited a decrease in T_g from 50 ^oC to 32 ^oC when saturated. After drying, a slightly higher T_g (57 ^oC) was observed; this was higher than the T_g that was previously measured for the dry material. The glassy modulus of the two epoxy systems was also observed to decrease when saturated. In the case of Epoxy B, the original glassy modulus was mostly recovered when the specimens were dried, whereas for Epoxy A, the glassy modulus for the specimens that were saturated and dried was lower than the original modulus.

As observed in Figures 8(c) and 9(c), the tan delta curves for the saturated epoxies also exhibited interesting characteristics. Both systems initially showed a single broad tan delta peak when dry that resolved into two separate peaks when saturated. After drying, two separate tan delta peaks were still observed, even though the T_gs had reverted back to their original dry values. If the large breadth of the tan delta peak suggests a heterogeneous structure, then it is possible that different components of that structure interact with water in different ways. For example, in addition to the chemical crosslinks in the network, attachments between the network and the filler may act as physical crosslink points. The sorption of water may perturb one but not the other. Another possibility is that the sorbed moisture plasticizes the resin and increases local mobility, thus allowing additional phase separation of the different components to occur. The

peaks corresponding to the components would become more distinct and such changes may persist after the water is removed. In any case, it is evident that the effects of moisture were not fully reversible upon desorption within the time scale studied here, and that changes in the polymer network structure had occurred due to moisture sorption.

Time-Temperature Superposition

The well-known principle of time-temperature superposition [13] is based on the hypothesis that, for a viscoelastic material, changing the temperature in an experiment produces the same effect as shifting the time scale (or frequency range) over which the measurements are made. This relationship can be used by conducting tests at a variety of temperatures and frequencies and shifting the results until they superimpose, thus generating a master curve that predicts behavior over a wide range of times (or frequencies). If this relationship holds, the material is called *thermo-rheologically simple*. With real materials, this hypothesis is probably never completely true, thus any superposition is always an approximation. The key question is how good an approximation it represents. It has been shown that epoxies with simple chemistries superimpose surprisingly well while more complex formulations may not [7]. The usual explanation is that these formulated materials are mixtures of epoxies and curing agents. Unless the various components in the cured material have the same temperature dependence, perfect superposition is difficult to achieve.

Figures 10(a, b) and 11(a, b) show the dynamic mechanical master curves for Epoxies A and B, respectively, representing the predictions for behavior over an extended frequency range. Neither epoxy system was truly thermo-rheologically simple, which is not surprising based on the earlier observation that the network structure appeared to be complex. Epoxy A showed more deviation from simple behavior than Epoxy B. This is particularly evident in the tan delta curves which seemed to be the most sensitive to the

quality of superposition.

Figures 10(c) and 11(c) show horizontal shift factor plots that indicate how much the data at each temperature must be shifted to obtain superposition. At temperatures well above the T_g, the curves normally show curvature which is concave upward displaying behavior described by the well-known Williams-Landel-Ferry (WLF) equation [14]. Below T_g, the plots are concave downward due to the so called physical aging effect [7]. The plots in Figures 10 and 11 show some tendency toward this behavior but seem to have a more complicated structure. This is particularly evident with Epoxy A where the curve appeared to have two transitions. This is consistent with the suggestion of a double peak in the tan delta curve.

Despite the deviations from thermo-rheologically simple behavior shown in Figures 10 and 11, further analysis can provide general trends. Because the creep behavior of these materials is of interest, the creep compliance curves for the two epoxies were calculated and shown in Figure 12. In light of the discussion above, this is in no way a substitute for the direct measurement of creep behavior; however, it is useful in determining the appropriate test conditions for measuring creep and identifying behavior of interest. As shown in Figure 12, the short time responses look similar as would be expected, but soon the curves begin to diverge. The difference between the curves grows, and eventually, the effect of the lower rubbery plateau modulus of Epoxy A in promoting creep can be seen.

In considering these curves, however, there is an additional factor contributing to the uncertainty in the superposition that must be considered. Because these materials are used at room temperature, it is useful to take 20 ^{o}C as a reference temperature. Unfortunately, this is in a range where the dynamic mechanical property curves (E', E", and tan delta) are rather flat for Epoxy B. This can be seen in Figure 11 by noting the

nearly horizontal tail at the high frequency end of all three curves. When generating master curves, shifting data that is nearly horizontal creates a degree of uncertainty because a range of options exists for curve overlap. The selection of optimum overlap, which is determined by operator judgment, controls the ultimate breadth of the time scale for the creep compliance curve. This is a much bigger issue for Epoxy B since Epoxy A does not show the same nearly horizontal tails at high frequencies.

To better estimate the uncertainly in predicted creep compliance behavior for Epoxy B, curve shifting was carried out using the maximum, average, and minimum shifts that could be selected based on the data. The resulting creep compliance curves and corresponding shift factor plots are shown in Figure 13. The most valid comparison to Epoxy A is with the Epoxy B average shift, which is roughly equal to the magnitude of shifting used for Epoxy A. However, the minimum and maximum shift creep compliance curves serve to bracket the range of potential behavior. All of the possible creep scenarios for Epoxy A showed more creep than indicated for Epoxy B. Although this creep is in the range of linear viscoelastic behavior, it may give some indication of expected behavior in the non-linear regime.

Temperature/frequency sweeps, which typically take > 9 h to complete, were not carried out on the saturated materials. The loss of moisture that would occur throughout the test would cause the viscoelastic properties of the material to continually change and compromise the quality of data and make it difficult to construct master curves. However, based on prior knowledge of the effects of moisture on the mechanical properties of glassy polymers, it is possible that the creep behavior observed in the dry specimens would be accentuated in the presence of moisture. Feng et al. have shown the equivalence between temperature and moisture in the creep behavior of a model epoxy system, which had a similar viscoelastic response at a higher temperature when dry as it

did at a lower temperature when saturated [15]. This showed that the presence of sorbed moisture can initiate the same creep response as in observed under dry, elevated temperature conditions.

Summary and Preliminary Conclusions

Detailed knowledge of the chemistry and network structure of these epoxy systems are too limited to draw specific and definite conclusions. However, the following observations and preliminary hypotheses are offered to guide additional study in this area:

- There are indications that Epoxy A, which was formulated with an accelerator and a different curing agent system than Epoxy B, may be under-cured when processed at ambient temperature. FTIR analysis revealed the presence of residual epoxide in Epoxy A, which disappeared following elevated temperature post-curing; no such peak was observed in the FTIR analysis of Epoxy B. DMTA temperature sweep experiments with Epoxy A showed an increase in the rubbery plateau as the test temperature increases. On the other hand, extended excursions above T_g, such as encountered during DSC analysis and a separate post-curing procedure carried out at 60 ^{o}C, resulted in a lower T_g rather than higher.

- In DMTA temperature sweeps, Epoxy A had a broader glass transition region with the suggestions of two overlapping transitions. This indicates that Epoxy A had a more complex and heterogeneous structure than Epoxy B. Another difference is that while the glassy moduli of the two systems are similar, Epoxy A had a significantly lower rubber plateau modulus than Epoxy B. A number of

factors could be responsible for this, for example, lower filler content or lower cross-link density. This lower plateau modulus in Epoxy A could potentially influence long-term creep.

- Onset of mass loss occurred at a lower temperature for Epoxy A as compared to Epoxy B. This mass loss could be attributed to the presence of non-reacted or non-network chemical species that are volatile and easily removed. It is hypothesized that these species are related to the accelerator, which is present in Epoxy A but not in Epoxy B, and/or to the differences in curing agent formulation.

- Moisture sorption at ambient temperature resulted in plasticization and T_g depression from ≈ 50 ^{o}C for both systems to ≈ 15 ^{o}C for Epoxy A and ≈ 32 ^{o}C for Epoxy B. A second transition was also observed in E', E" and tan delta of the saturated materials. The saturated T_g of Epoxy A was below room temperature, making it a rubbery material under ambient conditions, whereas the saturated T_g of Epoxy B was above room temperature. Moisture effects were observed to be not fully reversible upon drying.

- Temperature-frequency sweep experiments were carried out to examine the applicability of superposition. Neither of the epoxies was truly thermo-rheologically simple so the resulting master curves are only rough approximations, with Epoxy A exhibiting more deviation from simple behavior than epoxy B. Nevertheless, the master curves were used to estimate creep compliance for the two epoxies. While not a substitute for the direct

measurement of creep, the estimated curves indicate the type of behavior that should be explored in creep testing. The results suggest that Epoxy A will exhibit more creep than Epoxy B. Although the exact magnitude of this difference is complicated by the uncertainty in the predicted creep compliance for Epoxy B, all of the possible creep scenarios for Epoxy B showed less creep than that indicated for Epoxy A. Although this creep was within the range of linear viscoelastic behavior, it may give some indication of the behavior in the non-linear range.

Table 1: Summary of thermal analysis data from differential scanning calorimetry (DSC), dynamic mechanical thermal analysis (DMTA) and thermogravimetric analysis (TGA)

Temperature (^{o}C)	**Epoxy A**	**Epoxy B**
DSC		
First heat T_g	48.3 ± 1.3	54.9 ± 1.0
First cool T_g	41.5 ± 2.0	53.5 ± 0.3
Second heat T_g	43.6 ± 2.7	53.8 ± 2.1
Second cool T_g	41.32 ± 2.8	53.3 ± 0.3
DMTA T_g (E'' peak)	50.3 ± 1.5	52.2 ± 0.9
TGA – onset of mass loss	75 ± 1.2	115 ± 1.0

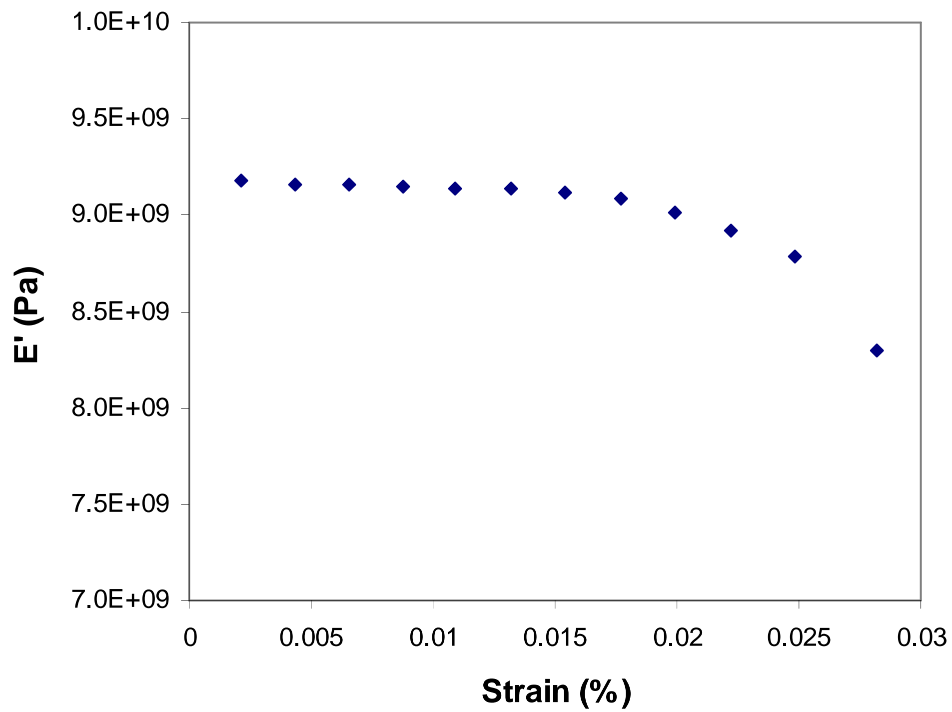

(a)

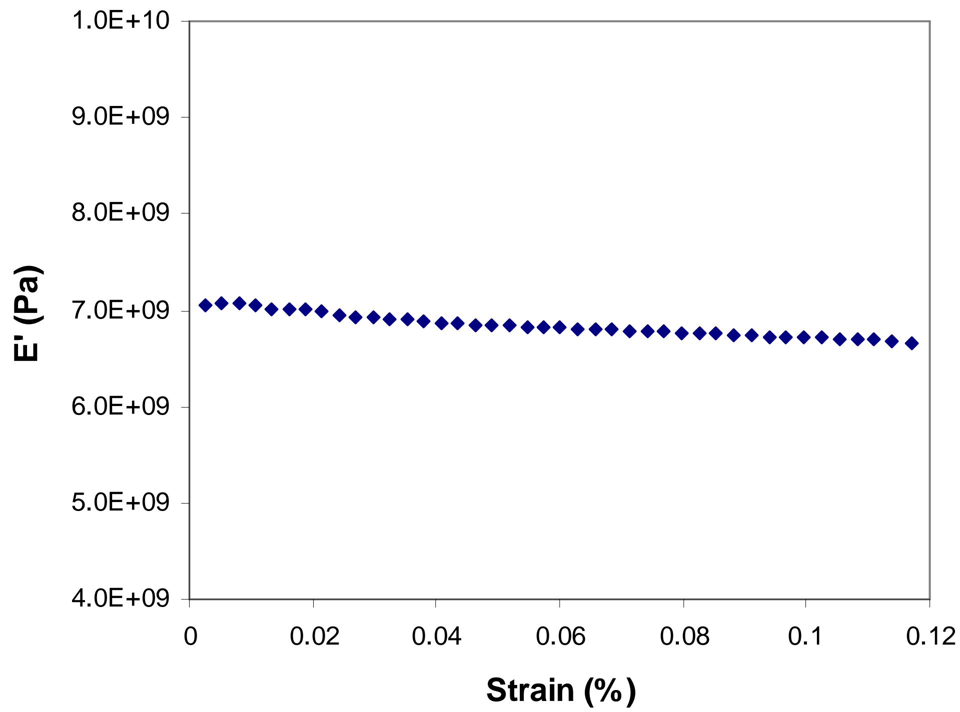

(b)

Figure 1: Representative DMTA strain sweeps for (a) Epoxy A, and (b) Epoxy B at room temperature.

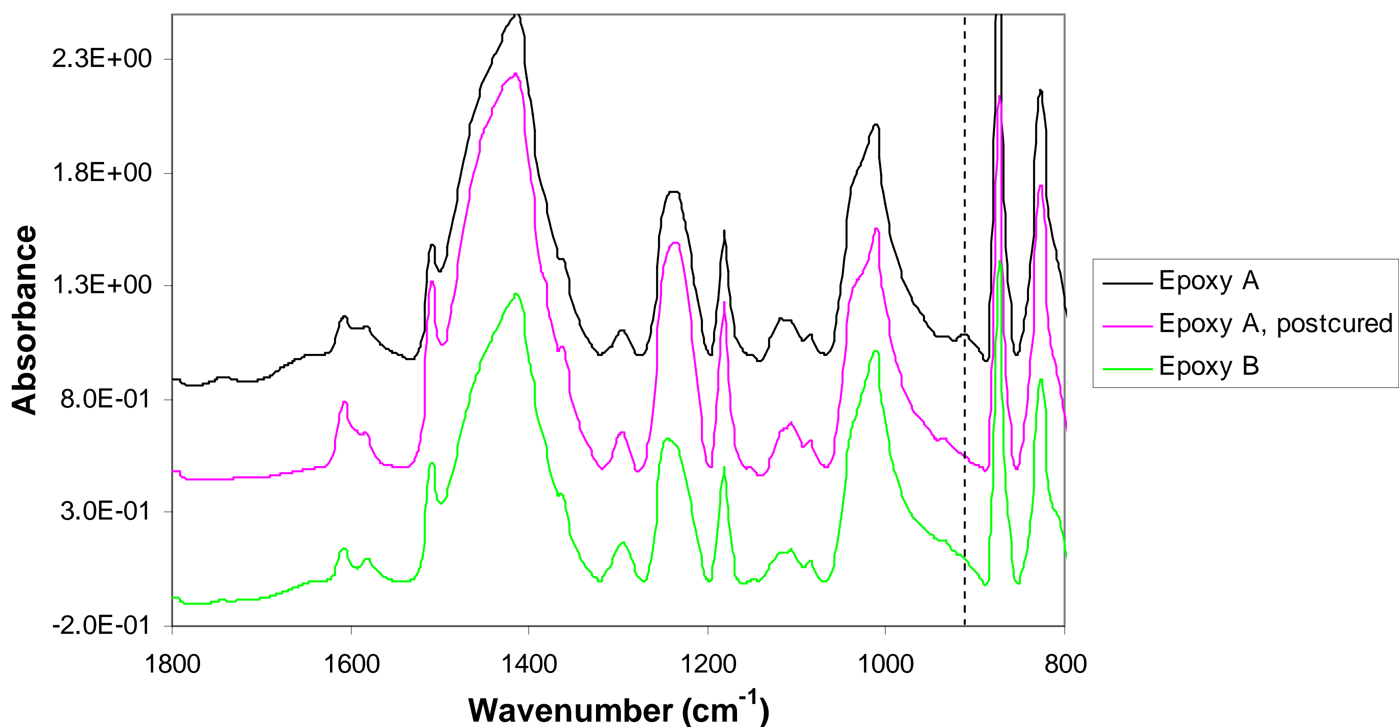

(a)

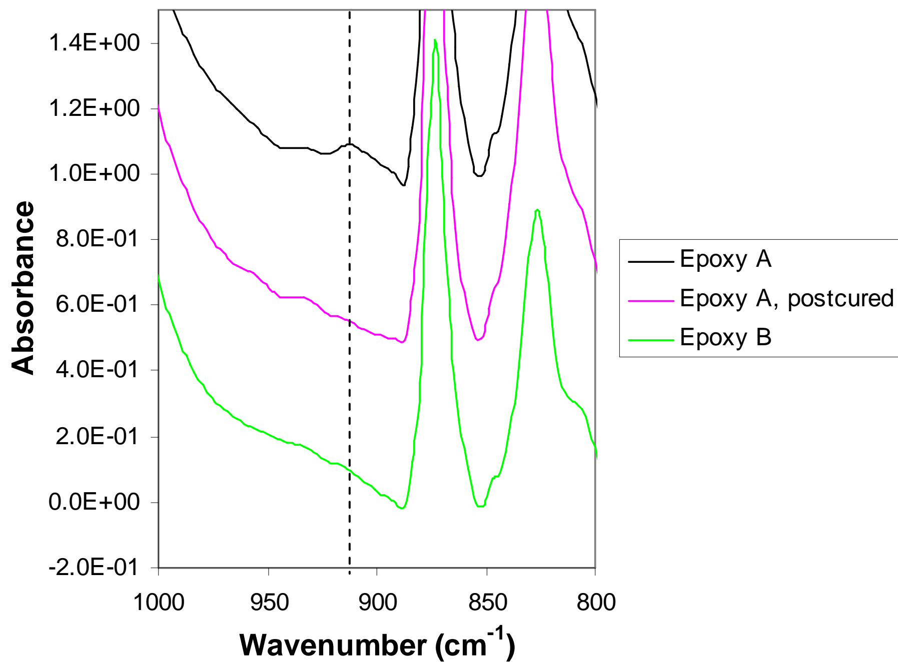

(b)

Figure 2: FTIR spectra of Epoxy A, Epoxy A postcured, and Epoxy B, showing location of epoxide ring peak at 911 cm^{-1} (dashed line).

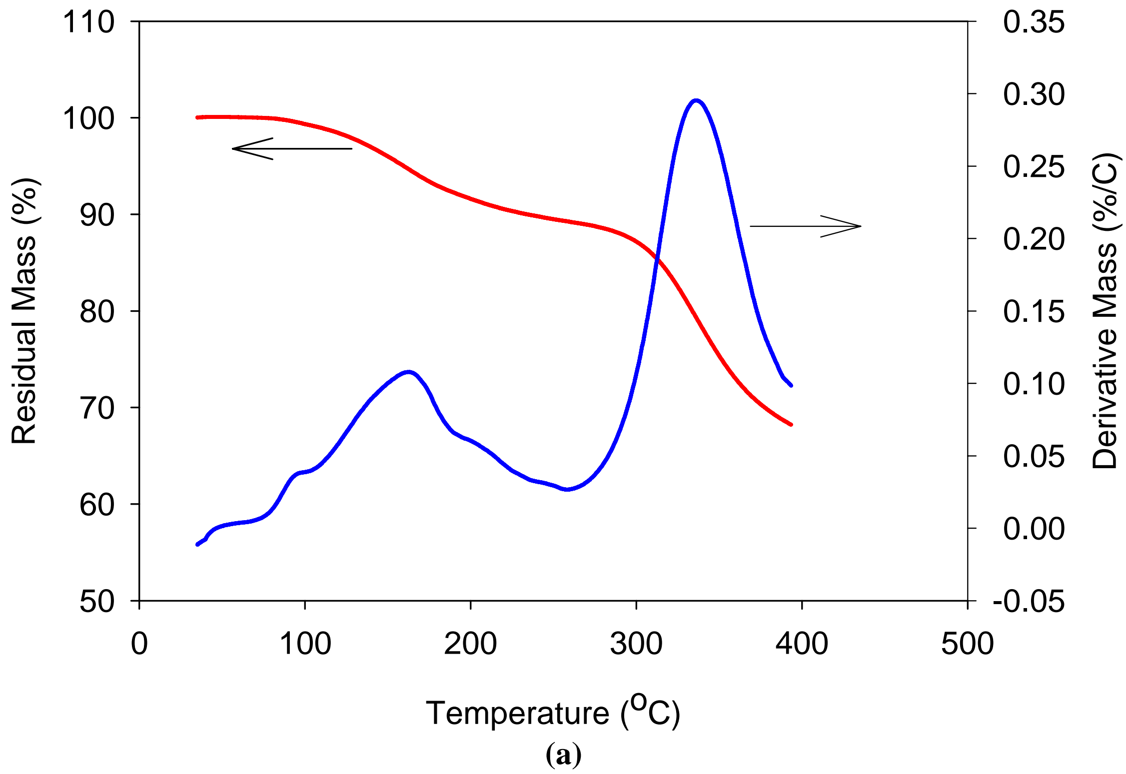

(a)

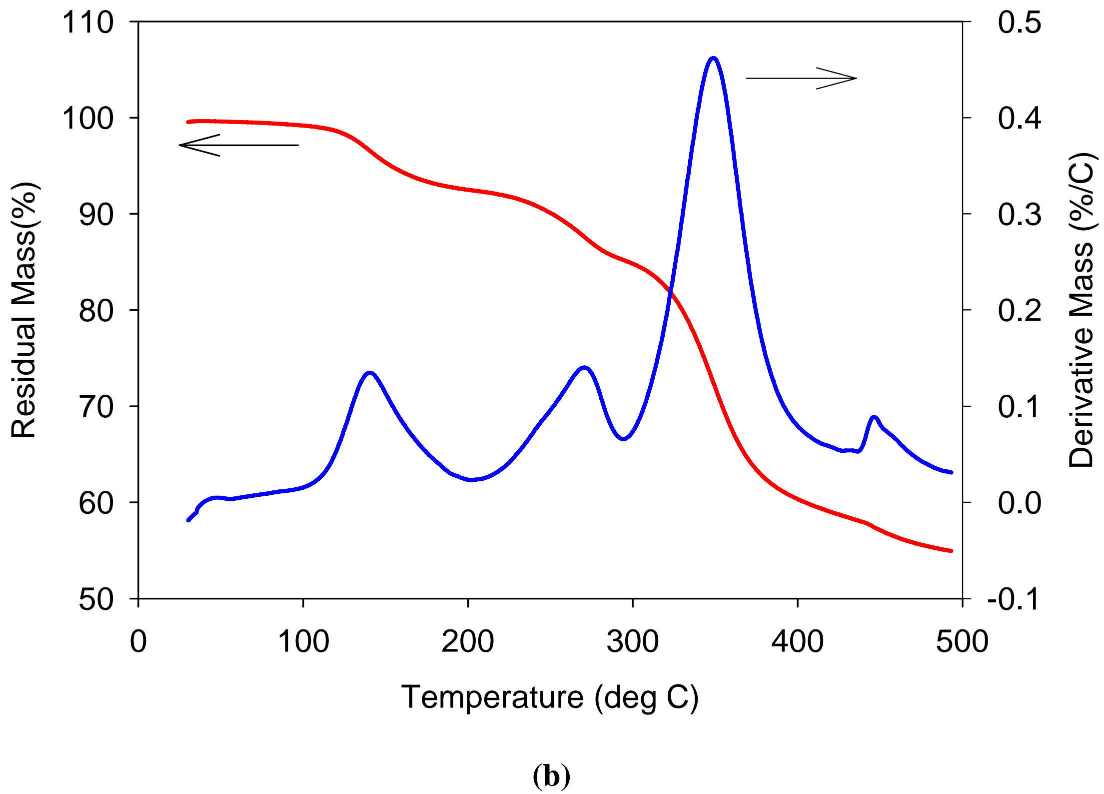

(b)

Figure 3: Representative TGA curves for (a) Epoxy A, and (b) Epoxy B, showing residual mass curve and derivative curve for residual mass as a function of temperature.

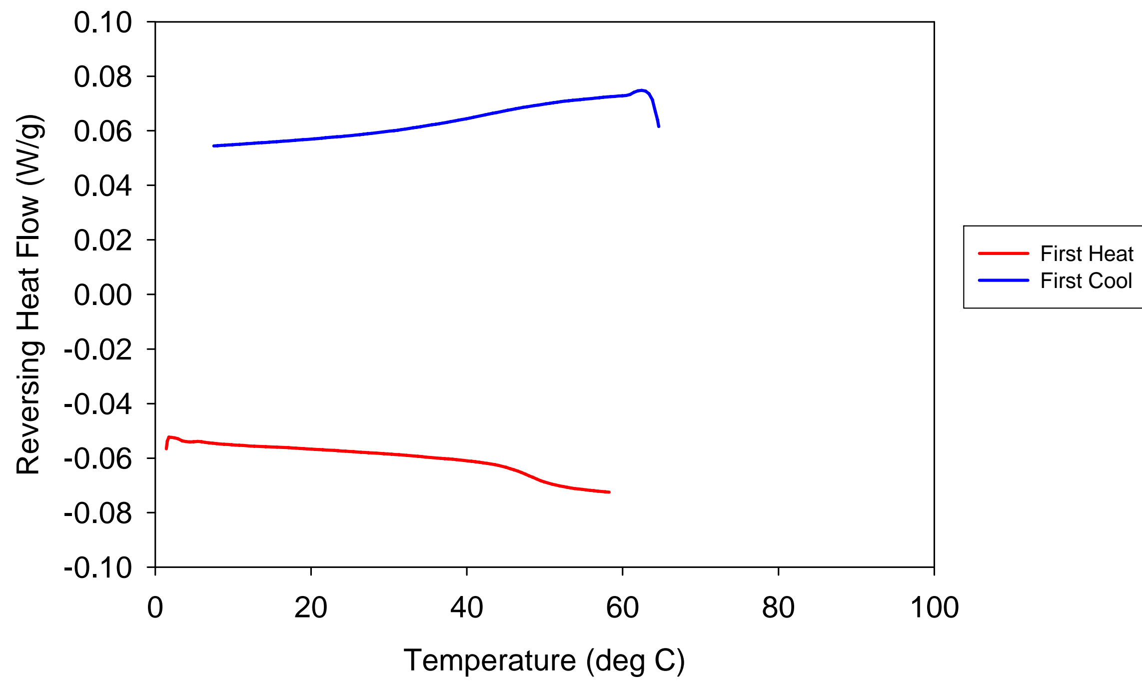

(a)

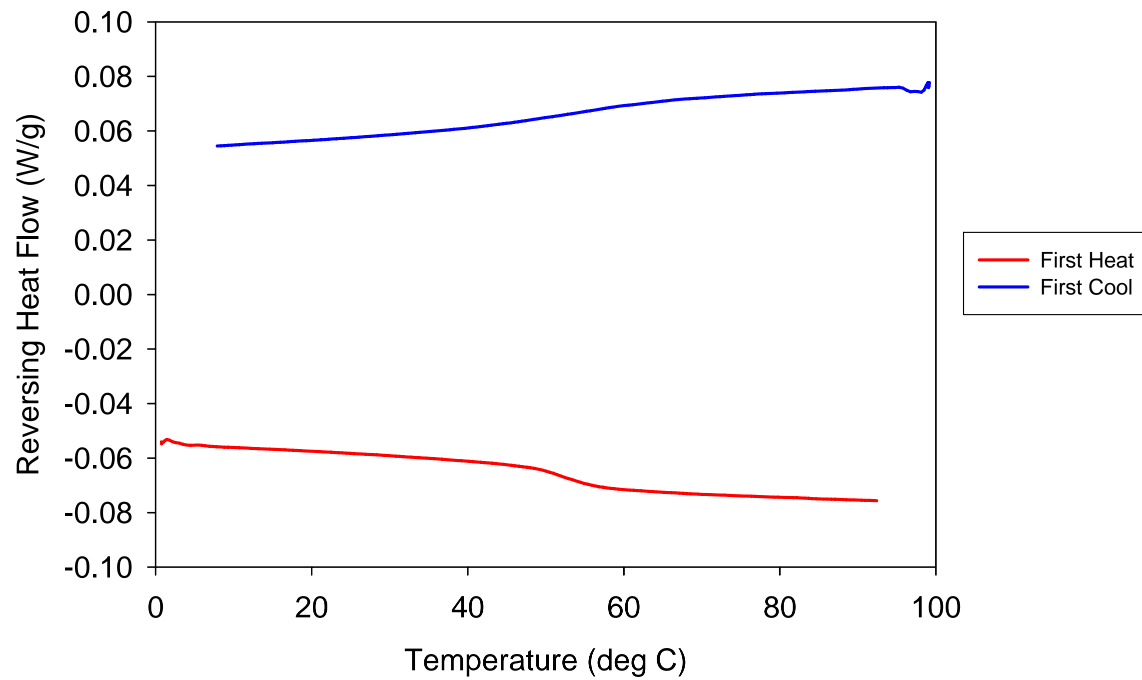

(b)

Figure 4: Representative modulated DSC curves for (a) Epoxy A and (b) Epoxy B, showing reversing heat flow for the first heating and cooling cycles.

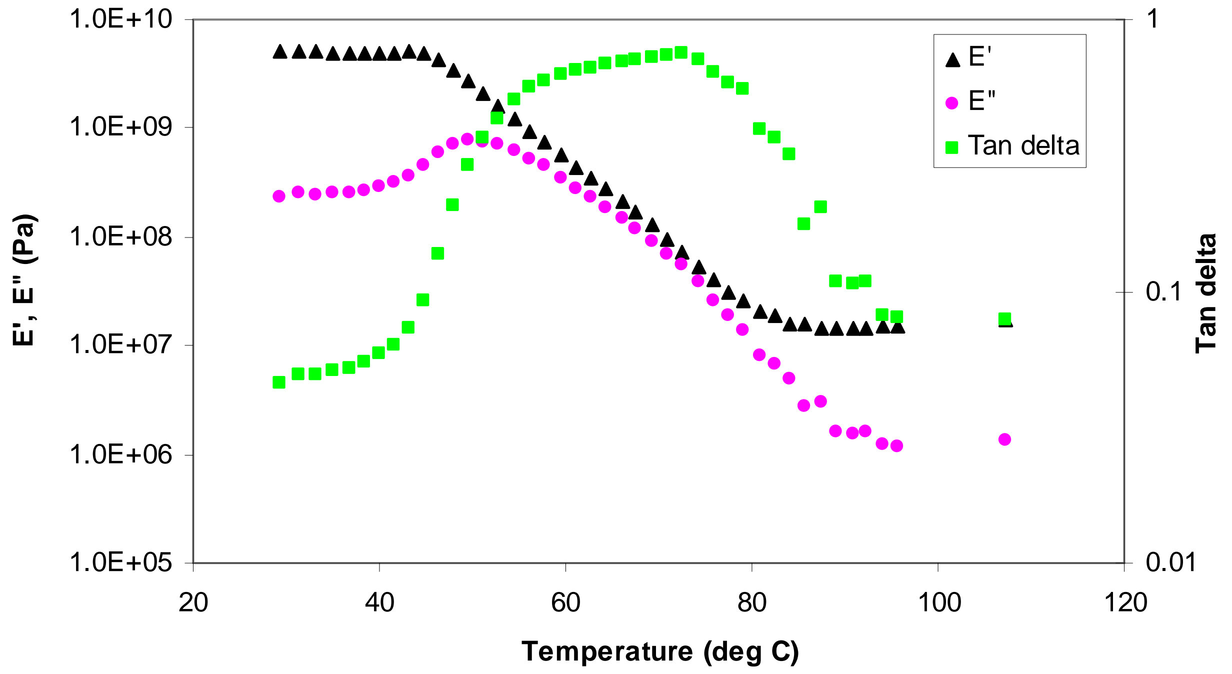

(a)

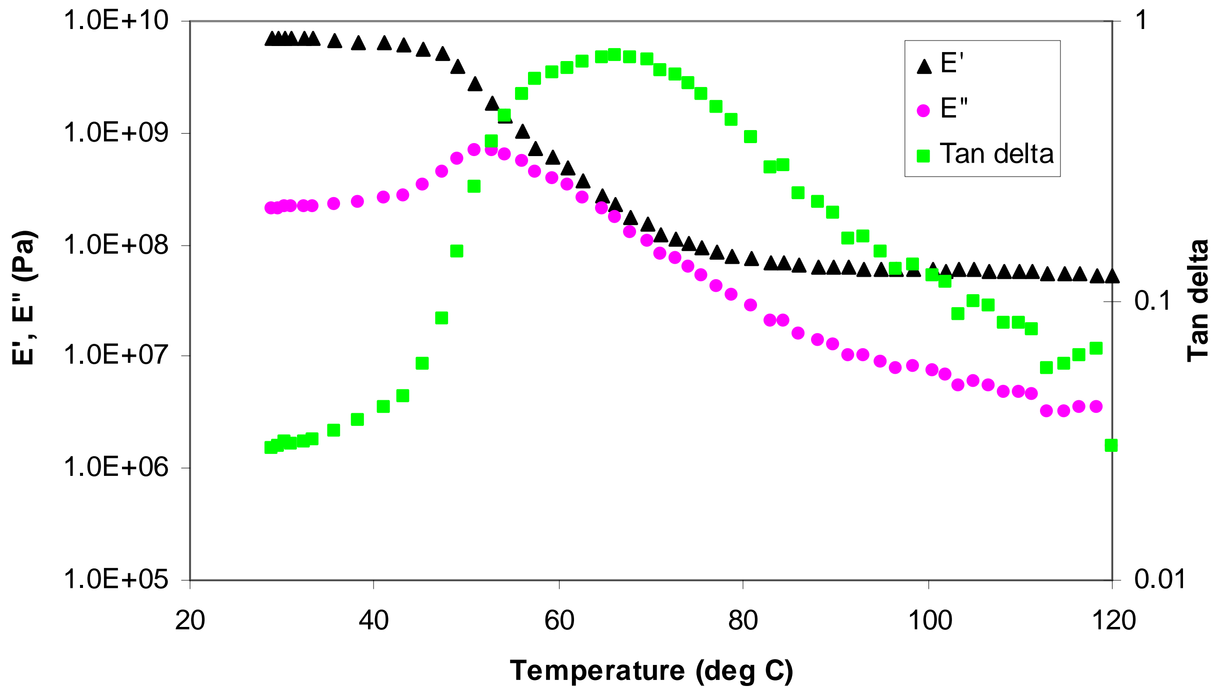

(b)

Figure 5: Representative E', E" and tan delta curves for (a) Epoxy A, and (b) Epoxy B, obtained at 5 Hz and 0.01 % strain.

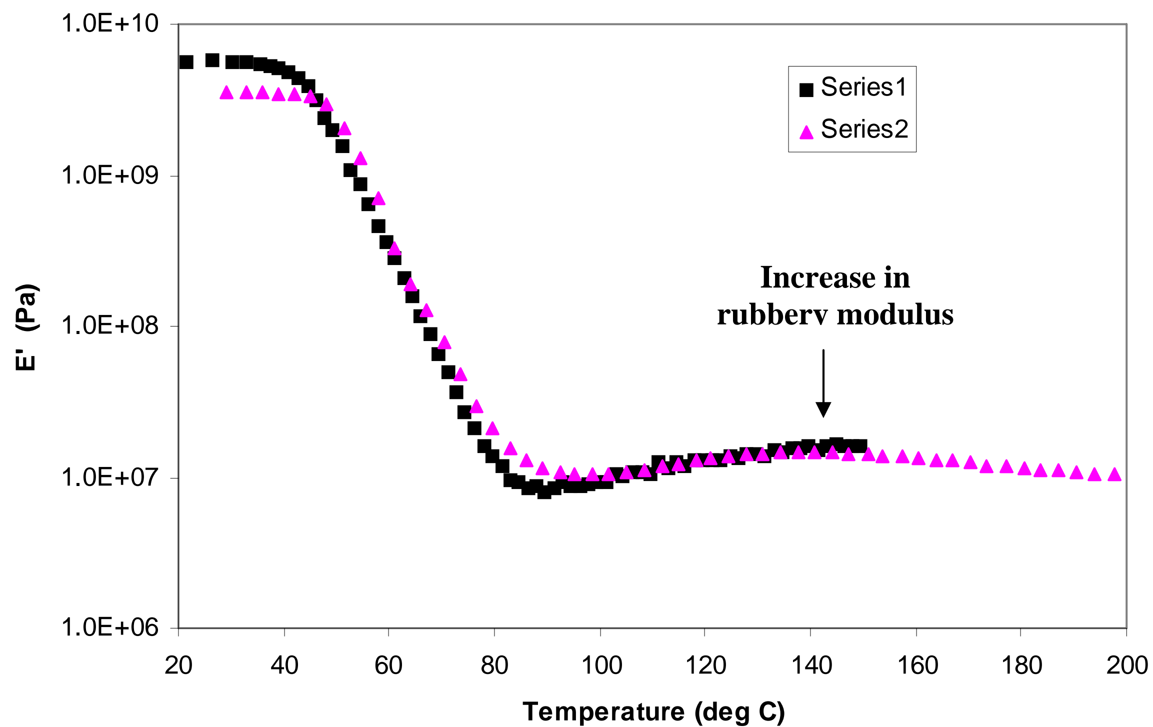

Figure 6: E' curve for Epoxy A, obtained at 5 Hz and 0.01 % strain, showing increase in the modulus in the rubbery plateau region as temperature is increased. Series 1 and Series 2 are two different Epoxy A specimens.

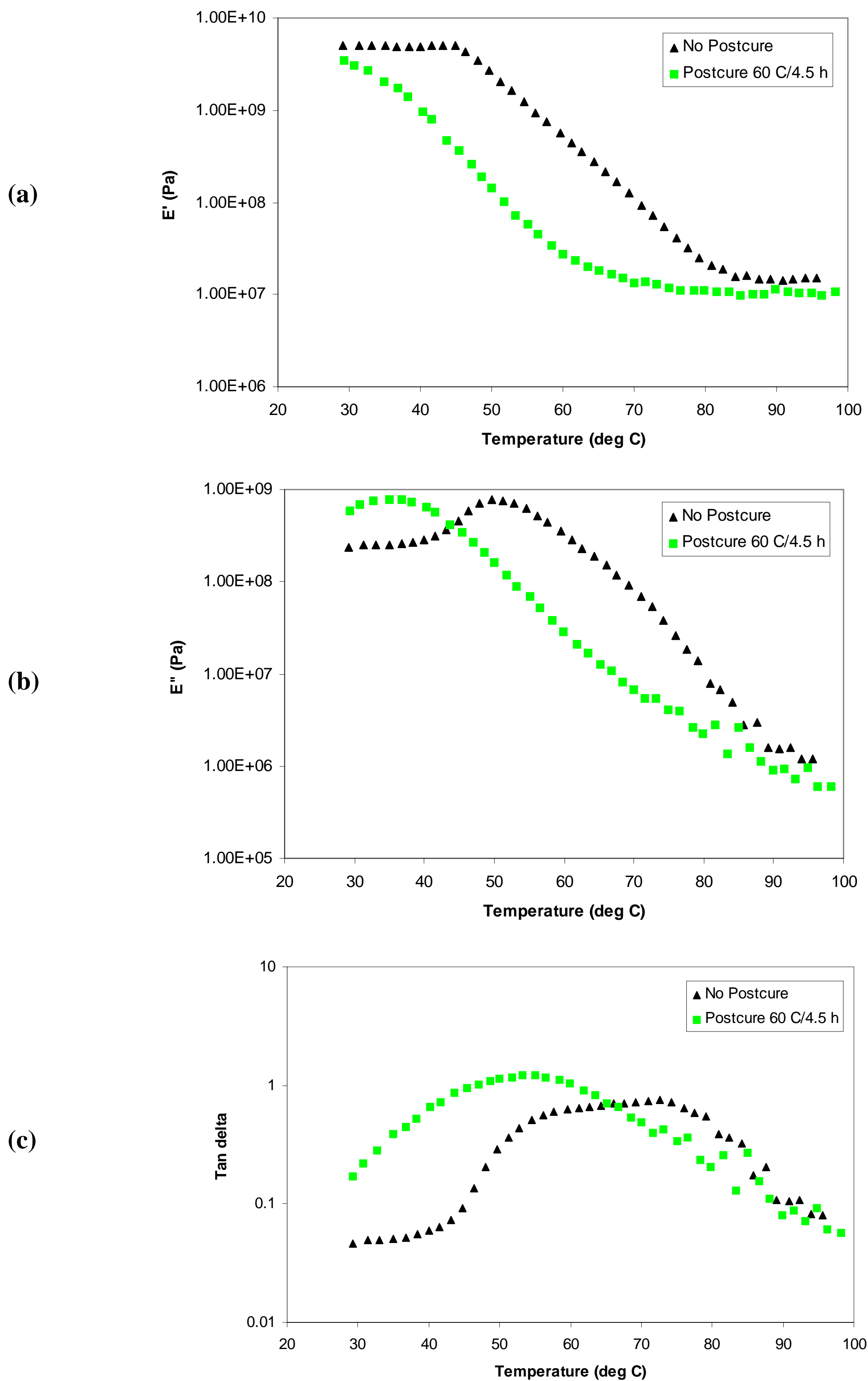

Figure 7: (a) E’, (b) E”, and (c) tan delta curves for Epoxy A prior to and following elevated temperature postcure, obtained at 5 Hz and 0.01 % strain.

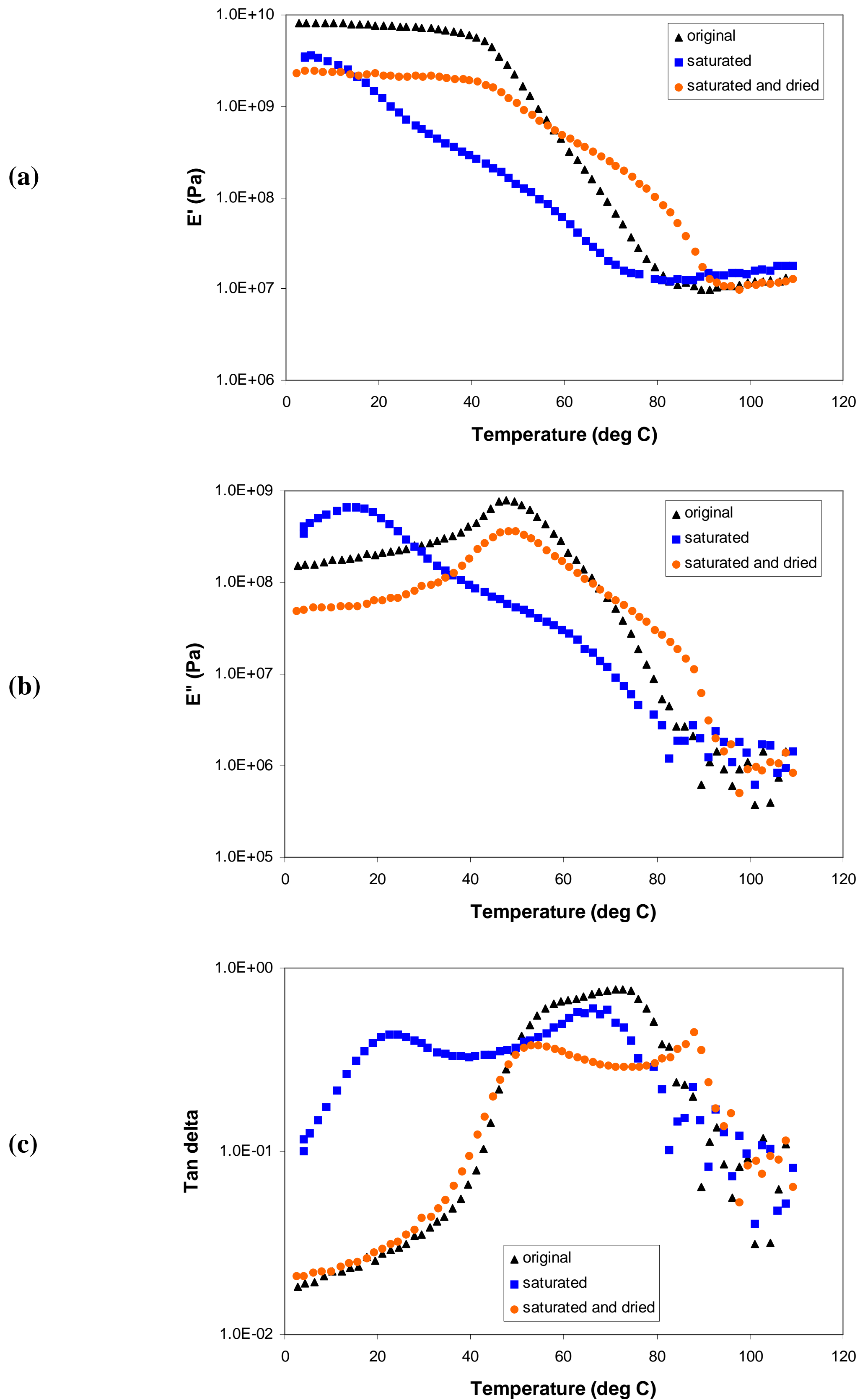

Figure 8: Comparison of (a) E', (b) E", and (c) tan delta curves for Epoxy A prior to moisture saturation, following saturation, and following saturation and drying, obtained at 5 Hz and 0.01 % strain.

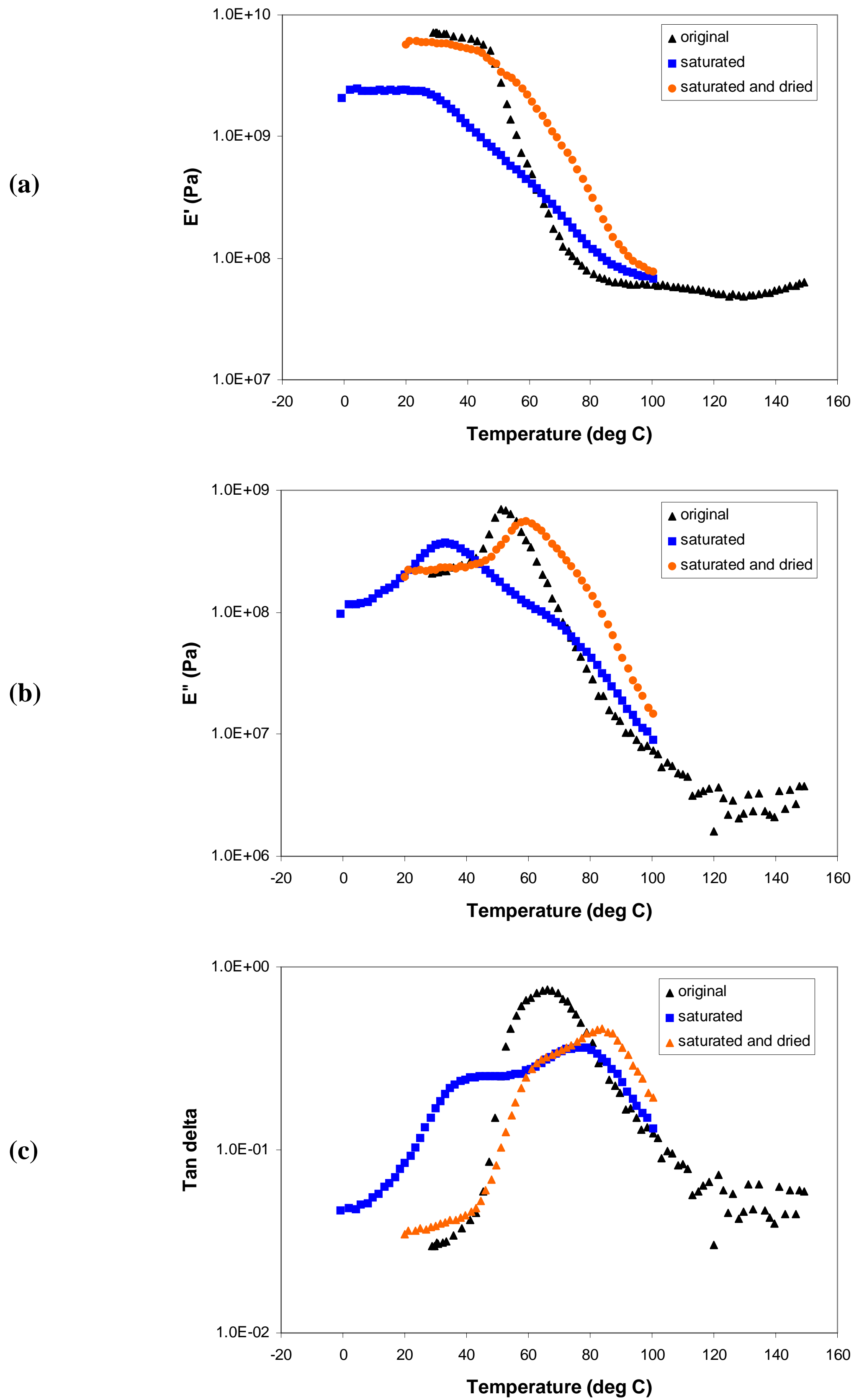

Figure 9: Comparison of (a) E', (b) E", and (c) tan delta curves for Epoxy B prior to moisture saturation, following saturation, and following saturation and drying, obtained at 5 Hz and 0.01 % strain.

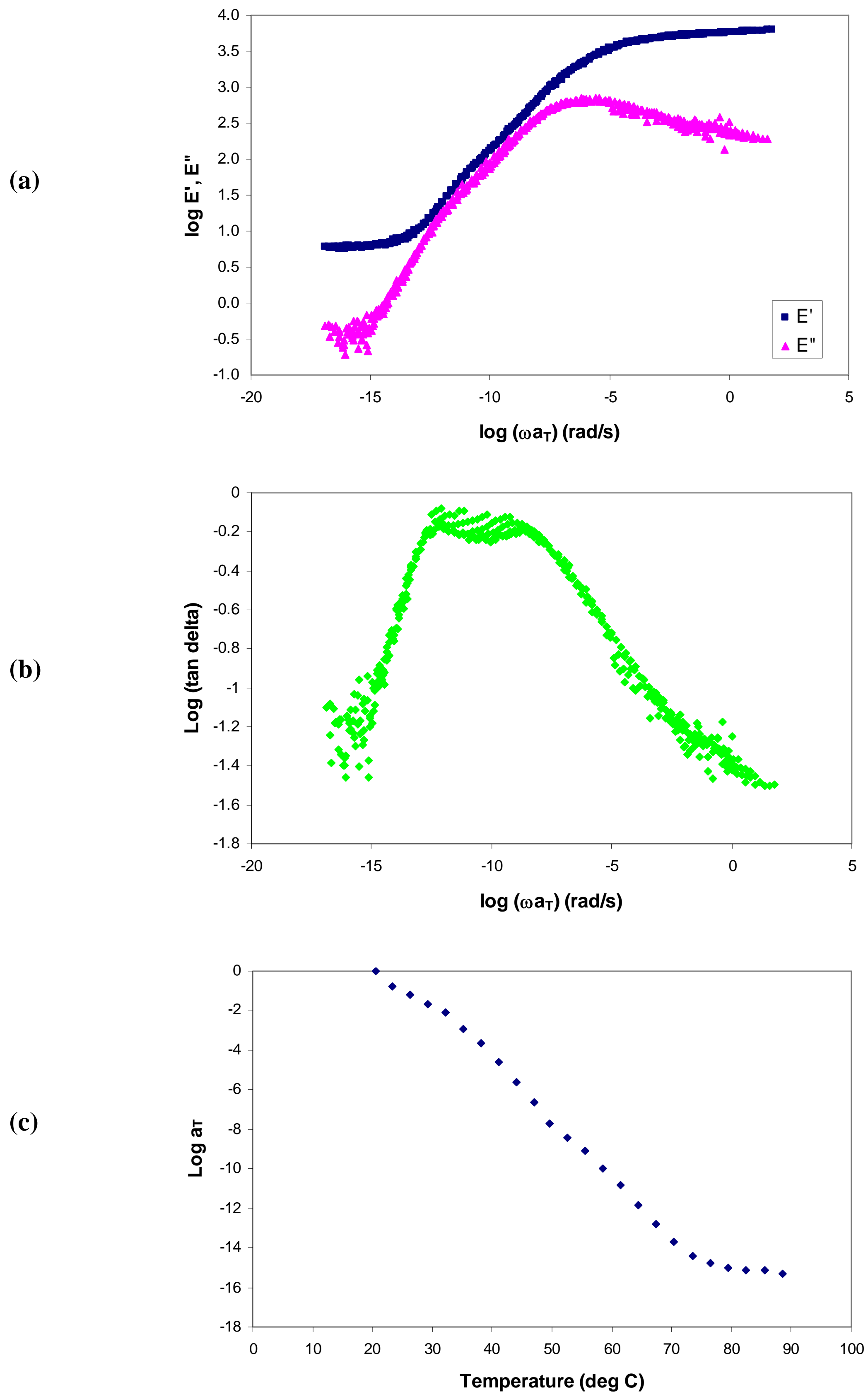

Figure 10: (a) E' and E" master curves, (b) tan delta master curve, and (c) shift factor plot for Epoxy A, obtained from frequency-temperature sweeps at 5 Hz and 0.01 % strain, referenced to 20 ^{o}C.

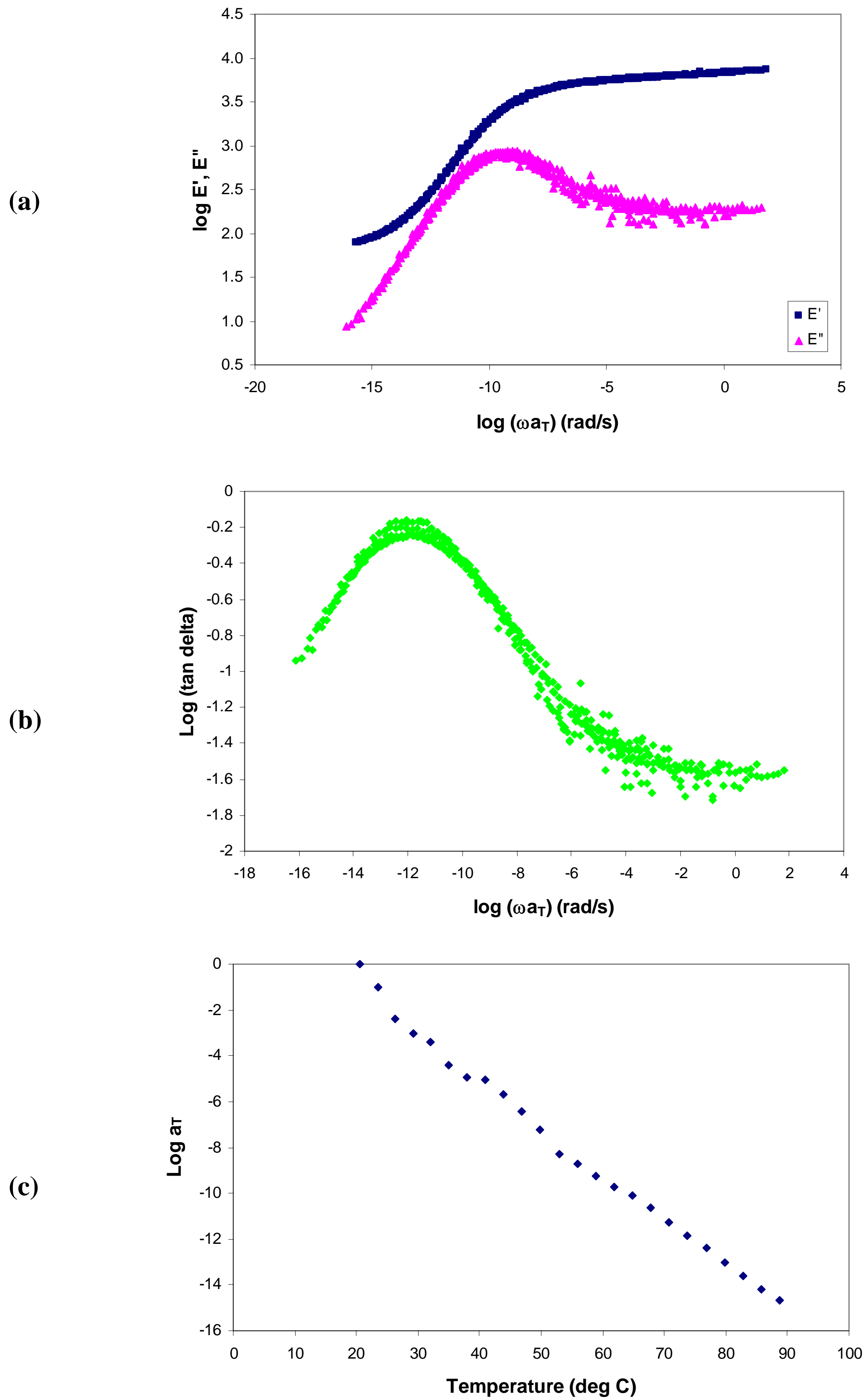

Figure 11: (a) E' and E" master curves, (b) tan delta master curve, and (c) shift factor plot for Epoxy B, obtained from frequency-temperature sweeps at 5 Hz and 0.01 % strain, referenced to 20 °C.

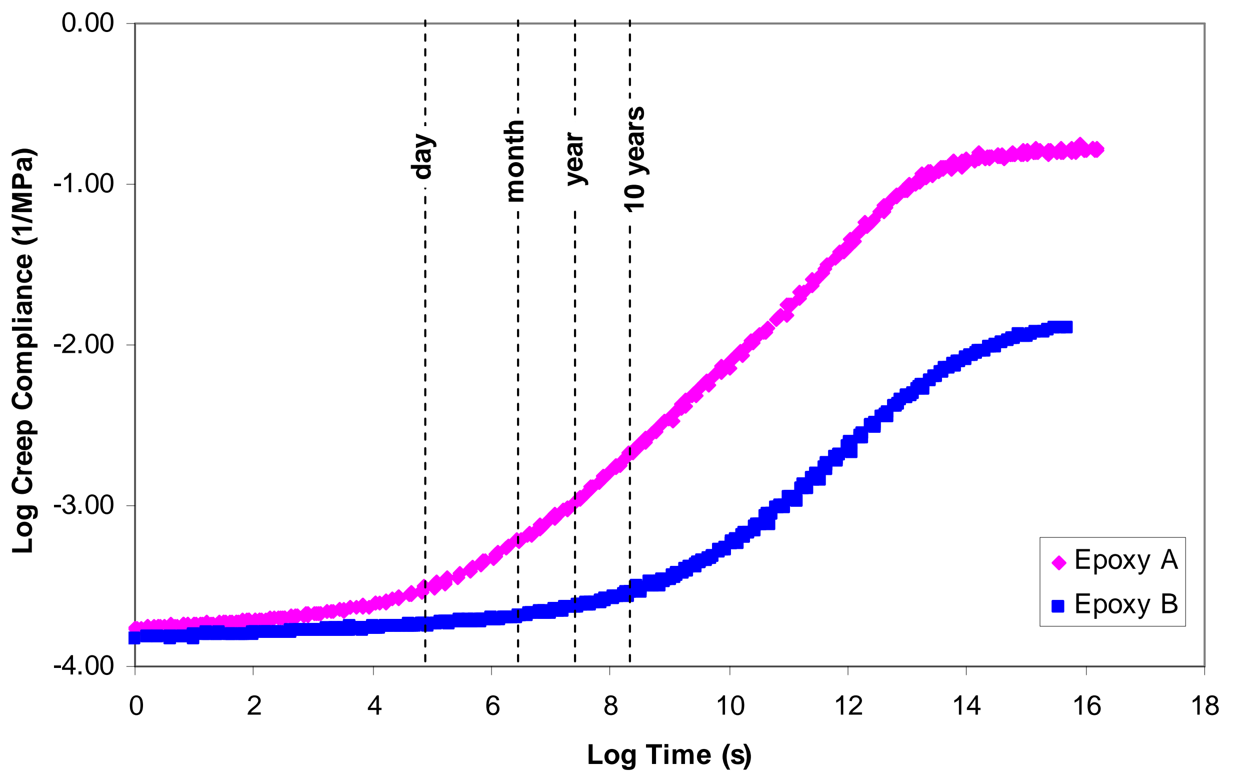

Figure 12: Comparison of estimated creep compliance for Epoxy A and Epoxy B, referenced to 20 °C, obtained from frequency-temperature sweeps at 5 Hz and 0.01 % strain, referenced to 20 °C.

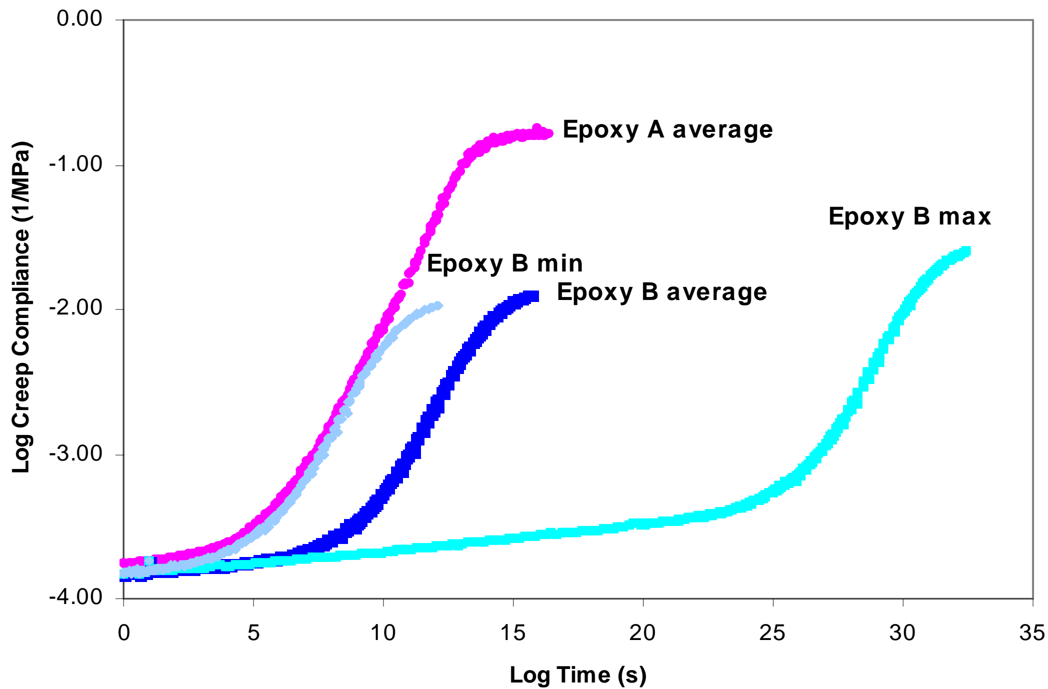

(a)

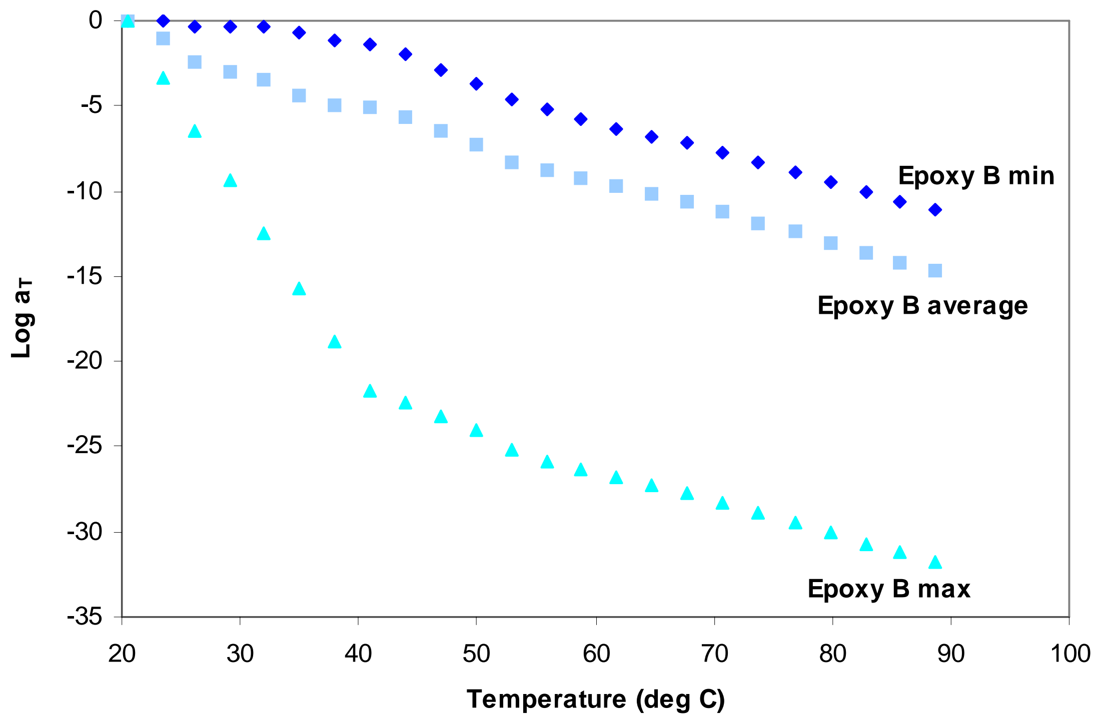

(b)

Figure 13: (a) Estimated creep compliance of Epoxy B for conditions of minimum, average and maximum curve shifting, compared to average shifting for Epoxy A, and (b) shift factor plots for Epoxy B for conditions of minimum, average and maximum curve shifting, obtained from frequency-temperature sweeps at 5 Hz and 0.01 % strain, referenced to 20 ^{o}C.

References

[1] R.A. Cook and R.C. Konz, "Factors Influencing Bond Strength of Adhesive Anchors", ACI Structural Journal, pp. 76-86, Jan-Feb 2001.

[2] V.M. Karbhari, M. Engineer, D.A. Eckel II, "On the durability of composite rehabilitation schemes for concrete: Use of a peel test", *J. Mater. Sci*., **21**, 147-156 (1997).

[3] G.L. Steckel, G.F. Hawkins and J.L. Bauer, "Environmental Durability of Composites for Seismic Retrofit of Bridge Columns", *Proceedings of the 2nd International Conference on Composites in Infrastructure*, H. Saadatmanesh and M.R. Ehsani, eds., 1998.

[4] J. K. Gillham and J. B. Enns, "On the Cure and Properties of Thermosetting Polymers using Torsional Braid Analysis," *Trends in Poly. Sci.,* **2**(12), 406-418 (1994).

[5] D. T. Behm and J. Gannon, "Epoxies", *in Engineered Materials Handbook, vol 3: Adhesive and Sealants*, pp. 94-102 (ASM International, 1990).

[6] ASTM E1640-04, "Standard Test Method for Assignment of the Glass Transition Temperature By Dynamic Mechanical Analysis"

[7] D.L. Hunston, W. Carter and J.L. Rushford, "Mechanical Properties of Solid Polymers as Modeled by a Simple Epoxy", Chap. 4 in *Developments in Adhesives – 2* , A.J. Kinloch, ed. (Applied Science Publishers Ltd., London, 1980).

[8] K. Ninomiya and J.D. Ferry, "Some approximate equations useful in the phenomenological treatment of linear viscoelastic data*", J. Colloid Sci*., **14**, 36 (1959).

[9] S. Farifa and A. Bouazzi, "Glass transitions in crosslinked epoxy networks: Kinetic aspects", *J. Thermal Analysis*, **48**, pp. 297-307 (1997).

[10] R.E. Cohen and A.R. Ramos, "Homogeneous and Heterogenous Blends of Polybutadiene, Polyisoprene, and Corresponding Diblock Copolymers, *Macromolecules*, **12**(1), 131-134 (1979).

[11] D.Y. Perara, "Effect of pigmentation on organic coating characteristics", *Prog. Org. Coatings*, **50,** 247-263 (2004).

[12] L.R.G. Treloar, *The Physics of Rubber Elasticity*, 3rd ed. (Clarendon Press, 1975).

[13] J.D. Ferry, *Viscoelastic Properties of Polymers* (John Wiley and Sons, New York, 1980).

[14] M.L. Williams, R.F. Landel and J.D. Ferry, “The temperature dependence of relaxation mechanisms in amorphous polymers and other glass-forming liquids”, *J. Amer. Chem. Soc*., **77**, 3701-3706 (1955).

[15] C.-W. Feng, C.-W. Keong, Y.-P. Hsueh, Y.-Y. Wang, H.-J. Sue, “Modeling of long term creep behavior of structural epoxy adhesives”, *Int. J. Adhes. Adhes*., **25**, 427-436 (2005).